FACTORS AFFECTING STRESS-INDUCED DEFECT GENERATION IN TRENCHED SOI FOR HIGH-VOLTAGE APPLICATIONS

W.A. Nevin, K. Somasundram, P. McCann, X. Cao and S. Byrne

Analog Devices Belfast Ltd., 5 Hannahstown Hill, Belfast BT17 0LT, N. Ireland, UK

ABSTRACT

This work investigates the effect of arsenic buried implants, as well as examining various structural and material aspects of slip dislocation generation in trenched and refilled fusion-bonded silicon-on-insulator (SOI) structures. We found that the implant concentration has a large impact on the ease of slip generation from the corners of filled trenches. For the same oxide liner thickness, slip occurred in samples with a dose of $5x10^{15}$ ions/cm^2, while no slip was seen in unimplanted SOI or with a $3x10^{13}$ ions/cm^2 dose. The enhanced slip appears related to the presence of a band of crystalline precipitates observed in high-dose implanted SOI, running parallel to the bonded interface at a level of about 50 nm above it. The nature and conditions of formation of these precipitates is discussed. The degree of slip generation was found to depend on a number of other parameters, including the material composition, SOI and oxide liner thicknesses, tub size, trench shape, and concentration of sidewall dopant.

INTRODUCTION

Trench-isolated fusion bonded silicon-on-insulator (SOI) is becoming an important commercial substrate for the fabrication of high-voltage electronic devices, used in areas such as telecommunications, displays and smart power (1,2). By trenching through the top layer to the buried oxide (BOX), and then lining the trench sidewalls with silicon oxide, electrically isolated tubs of silicon are formed, on which the devices can be fabricated. The technology gives a number of advantages over conventional dielectrically isolated substrates, including improved electrical performance, higher quality and versatility of the silicon layer type, lower bow/warp values, and substantial scope for die shrinkage. However, a major obstacle to extending the range of breakdown capability to higher voltages is the generation of slip dislocations in the SOI layer at filled trenches, during thermal cycling of the structures at high temperature. This occurs as a result of increasing levels of stress in the silicon along the trench sidewall with increasing thickness of the sidewall oxide. The stress is thought to originate from the difference in thermal expansion coefficient between silicon and its oxide, and peaks close to the bottom corners of the trenches, so that the slip generally emanates from these areas (2-5). Subsequently, slip lines propagating through the bulk of the SOI layer can result in degradation of the device performance, for example by acting as channels for dopant diffusion. To achieve the required high breakdown voltages, therefore, it has been necessary to either keep the oxide thickness below the threshold for slip generation and incorporate double or triple trench structures, or to design any sensitive device regions around the slip dislocations. However, both these solutions increase the size of the die area compared to what could be obtained in the absence of slip.

We recently reported (3) that the ease of generation of slip is strongly dependent on the doping type and doping concentration of the silicon material. In particular, the incorporation of high levels of arsenic or antimony during the silicon crystal growth resulted in considerable strengthening of the SOI layer compared to other dopants. In contrast to this, inserting a buried implanted layer of these dopants at the bottom of the SOI layer weakened the material, resulting in increased levels of slip generation from the bottom of filled trenches. This is an important characteristic, since a doped buried layer is typically included to improve the electrical performance of high-voltage devices fabricated on SOI (2), as well as acting as a getter to reduce oxygen-related defects and increase the minority carrier lifetime (6). In this work, we have used transmission electron microscopy (TEM) and secondary ion mass spectroscopy (SIMS), as well as other techniques, to examine the silicon structure and composition in the SOI region close to the bonding interface, with a view to elucidating the origin of this buried implant effect. In addition, we have further investigated the various structural and material aspects of slip generation in thick-film SOI. By controlling the composition of the silicon material and the pre-bond processing conditions of the device layer, we were able to achieve slip-free thick-oxide refilled trenched structures capable of withstanding high-temperature cycling without slip generation, even with the incorporation of high-dose buried implanted layers.

EXPERIMENTAL

Starting "device" materials used to form the SOI layers were polished 5" dia. (100) silicon Czochralski (CZ) and float zone (FZ) wafers with phosphorous doping and a resistivity of 3-15 ohm-cm. For the fabrication of SOI with buried implanted layers at the bonding interface, the device wafers were blanket-implanted before bonding with 30-80 keV As ions over a dose range of 3×10^{13}-5×10^{15} As ions/cm^2. This gave a layer with a dopant concentration of about 10^{17}-5×10^{19} atoms/cm^3 in the device close to the BOX interface, after the final stage of sample processing. The "handle" material was 3-5 ohm-cm phosphorous-doped polished CZ silicon with (100) crystal orientation. A 0.5-1.0 μm thick thermal oxide layer was grown on the handle wafers before bonding, which formed the BOX of the SOI wafer. The bonded SOI samples were prepared using the process described previously (6), by joining the device and handle wafers at room temperature following a modified RCA clean, and bond annealing at 1050ºC. The device layer was then thinned to 20-50 μm by grinding and chemical-mechanical polishing, patterned using standard photolithographic techniques, and 3 μm wide trenches etched to the buried oxide using an inductively coupled plasma etching method (7). The angle between the trench sidewall and the surface plane was close to 90º. After trenching, a phosphorous doped layer was diffused into the trench sidewalls by annealing the wafers with solid phosphorous sources. This gave a dopant concentration of around 10^{19}-10^{20} atoms/cm^3 near the sidewall surface after a thermal drive-in at 1050ºC.

Slip dislocation generation was examined by refilling the trenches and thermally stressing the samples by annealing at high temperature. The full refill process consisted of first lining the trenches with a thick layer of low-pressure chemical vapour deposited (LPCVD) TEOS (tetraethoxy silane) oxide deposited at 700ºC, then filling the centres with LPCVD polysilicon at 620ºC, planarising the polysilicon, capping the trench top with a further LPCVD oxide layer, and annealing at 1050ºC in nitrogen at two stages of the refill process (see Scheme 1). The thermal annealing resulted in densification and shrinkage of the oxide films by around 5%. The degree of generated slip during the refill was analysed by inspecting the SOI surface using phase-sensitive Nomarski optical microscopy, and at the end of the process by Secco etching of the surface and cross sections. Around five samples were processed in each group of wafers. The degree of slip was estimated as a percentage of die affected by slip, measured along two lines across the wafer diameter, perpendicular and parallel to the flat, bisecting at the wafer centre (one affected tub in a die constituted a positive count). The total number of die along these lines was 100, and the dimension of each die was about 1 mm square. To allow for an observed wafer-to-wafer variation, the slip was taken as the average of all the wafers in a given group. TEM, SIMS, energy dispersive X-ray spectroscopy (EDX), focussed ion beam (FIB) and atomic force microscopy (AFM) were carried out at QinetiQ, and scanning electron microscopy (SEM) at QinetiQ and Edinburgh University.

RESULTS AND DISCUSSION

Effect of Buried Implants and Sidewall Doping on Slip Generation in SOI

Table I lists the results of slip inspections at the processing stages of post TEOS oxide liner deposition, post liner densification and post final oxide densification, for samples prepared using different growth methods (CZ vs FZ) for the SOI layer silicon and with different doses of arsenic buried implant. The thickness of the oxide liner on the sidewall in each case was 0.6 µm. All samples were free of slip after the initial liner deposition, and the unimplanted wafers remained slip free throughout the entire refill and thermal annealing process. The implanted samples, in contrast, showed a sensitive dependence on both the material type and the implant dose. In the case of a low implant of 3×10^{13} ions/cm^2, both types of material behaved similarly to the unimplanted wafers, with no slip apparent. However, when the dose was increased to 5×10^{15} ions/cm^2, the FZ samples had severe slip after annealing of the TEOS liner. The slip dislocations are generated first in the high-stress region close to the bottom corners of the trenches. The dislocations then propagate up through the SOI layer along the Si (111) plane, and intersect the wafer surface as lines parallel to the trenches, which can be observed by a combination of surface Secco etching and Nomarski microscopy. A typical image is shown in Figure 1(a). On the other hand, the CZ wafers remained slip-free throughout the refill and annealing processing (see Fig. 1b). Clearly, therefore, there is much greater weakening of the silicon material in the case of the FZ material on incorporation of the high-dose buried implant. Secco etching of cross-sections of these samples confirmed the optical microscopic slip inspection results.

We used TEM to examine the structure of the SOI layer close to the bonding interface, and Figure 2 compares images for CZ samples with high and low level implanted layers. In the case of the high-implant sample, a band of precipitates is identified in the SOI layer, running parallel to the bonding interface, at a distance of about 50 nm above it, which is the region where the peak concentration of arsenic atoms is expected to lie immediately after implant. From the observed Moire fringes, as seen in Figure 2(c), the precipitates appear to be crystalline, and are about 8 nm in size. Similar precipitates were also seen in the high-implant FZ SOI layer. In contrast, no precipitates were found in the SOI with a low arsenic implant (see Fig. 2b), nor in the unimplanted samples. It is conceivable that the mechanical strength of the silicon in the region of these precipitates might be weakened, thus resulting in a lower threshold for slip formation. The difference in behaviour between the FZ and CZ material, may be due to the widely different oxygen content between the two types of silicon. Thus, the interstitial oxygen present in the CZ lattice might result in a strengthening of the silicon bonding structure, to either prevent the initiation of slip dislocations or inhibit their propagation through the silicon, and so counteract the weakening effect of the implant. In order to elucidate any variations in the chemical composition of the silicon in the region of the precipitates, a series of careful SIMS analyses was carried out across the area next to the BOX. Figure 3 shows the profiles of carbon and oxygen found in the CZ sample of Fig. 2(a), indicating peaks due to both carbon and oxygen in the region of the precipitates. In the case of the FZ material, a similar peak is again present for carbon, but not oxygen. EDX and SEM were used to ensure that the SIMS probe beam had not penetrated through the silicon layer to the oxide, while TEM, AFM and FIB were used to confirm the accuracy of the analysis depth. The estimated density of precipitates correlated closely with the carbon concentration measured by SIMS, indicating that the precipitates are probably silicon carbide. In addition, the observed accumulation of oxygen in the implant region in the CZ sample adds further evidence to its possible role in inhibiting slip dislocation generation at the trench bottom corners. Concerning the origin of the precipitates, we can speculate that carbon impurities might diffuse within the silicon lattice during the high-temperature bond anneal, and subsequently accumulate and react with silicon in the structurally modified regions where the arsenic ions have been implanted.

In conjunction with a buried implant, sidewall doping is often used to improve the electrical performance of trench-isolated high-voltage devices (2). Therefore, in view of the influence of the buried implant on slip, we also examined the effect of different levels of phosphorous diffused into the trench sidewalls on the generation of slip after liner deposition. The results are listed in Table II for samples prepared using CZ silicon material with a buried As implant of 1 x 10^{15} ions/cm^2 and a TEOS liner thickness of 0.8 μm. Here again, we see a strong influence of dopant level on the ease of slip generation from the trench bottom corners. While there is no occurrence of slip in the undoped and lightly doped samples, the degree of slip increases with increasing phosphorous dose above a level of around 10^{15} atoms/cm^2. Thus, the incorporation of the dopant atoms into the silicon in the region near the silicon-silica interface also results in a weakening of its structure, which in this case appears due to stress from the diffusion of a high concentration of phosphorous atoms into the silicon lattice.

Effect of SOI Structural Parameters on the Formation of Slip

We examined the effect of various SOI parameters on the degree of slip generation, including SOI thickness, TEOS oxide liner thickness, trench profile, and tub size. In particular, the SOI thickness was found to have a strong influence, as shown in the upper part of Table III for samples with a 0.9 μm thick oxide liner and no buried implant. Here, the degree of slip increased markedly when the SOI thickness was increased from 35 to 50 μm, while negligible slip was seen at 20 μm. This indicates that the stress causing slip at the trench bottom corner is an accumulation of the total stresses along the oxide liner/Si sidewall interface, which will therefore depend on the length of this interface. The second group of samples in Table III illustrates the effect of TEOS liner thickness on slip generation for 20 μm SOI with a similar structure (Type A). In the absence of a buried implant, little difference was observed between FZ and CZ material, and the onset of sufficient stress to generate slip occurred at around 1.2 μm oxide deposited on the Si trench sidewall. In contrast, for a thicker SOI with a high-dose buried implant and mask pattern with smaller tubs, the threshold for slip generation was found to occur at a much lower TEOS oxide thickness of only 0.25 μm, even when using CZ material (Type B in Table III). These results illustrate the cumulative and interactive effects of the various structural parameters, which need to be taken into consideration when attempting to predict slip behaviour in SOI.

The trench profile was also found to have a significant influence on slip generation, such that any undercutting or uneveness of the trench sidewall at the bottom of the trench resulted in increased slip, presumably as a result of increased stresses generated at the silicon spikes. For example, no slip was found for the trench profile of Figure 4(a), while severe slip occurred in the sample of Figure 4(b). Hence, the development of a dry etching process (7) which can produce a smooth trench profile with no undercutting of the silicon at the buried oxide is important for controlling slip in SOI.

In an attempt to extend the slip threshold of the most sensitive high-implant structures, we investigated various pre-bond annealing treatments of the implanted device wafers. Analysis by TEM for an optimised process found no precipitates in the implanted region, while SIMS profiling showed an absence of any carbon signal in the SOI near the BOX. In addition, the slip behaviour was greatly improved, with these samples remaining slip-free for a sidewall oxide thickness of 0.55 μm, which is twice the thickness achievable without the pre-bond treatment (see Table III). This gives further evidence linking the formation of the precipitates to the slip generation mechanism.

CONCLUSIONS

In this work, we have investigated the effect of arsenic buried implants, as well as examining various structural and material aspects of slip dislocation generation in trenched and filled SOI having thick sidewall TEOS oxide liners, for use in high voltage applications. The ease of slip generation from the trench bottom corners was found to be strongly dependent on the implant dose and silicon growth method, such that a combination of high-implant and FZ material resulted in severe slip formation, while CZ material remained slip-free, for a sidewall liner thickness of 0.6 μm. TEM identified the presence of a band of crystalline precipitates in the region of the high-dose buried implant, which appear to be silicon carbide from SIMS analysis. These may structurally weaken the silicon in this area, resulting in a lower threshold for slip generation. An observed accumulation of oxygen in the silicon in the same region may account for the strengthening of the CZ material compared to FZ in the presence of a high implant. The diffusion of high levels of phosphorous dopant into the trench sidewalls also lowered the threshold for slip generation, with the effect strongly dependent on the doping dose.

The degree of slip was found to increase with increasing SOI thickness, TEOS liner thickness and decreasing tub size, and was also strongly influenced by the quality of the etched trench sidewall at the trench bottom, where undercutting resulted in enhanced slip generation. Hence, the ease of slip formation depends on a complex interaction of a number of structural parameters. Whereas, with relatively thin (20 μm) unimplanted SOI it was possible to deposit around 1.2 μm of TEOS oxide on the sidewall without generating appreciable slip, 35 μm thick SOI with a high-dose buried implant and smaller tub size had a TEOS oxide threshold thickness of only 0.25 μm, even with CZ material. By developing a pre-bond device annealing process, we were able to double the slip threshold to more than 0.5 μm oxide thickness for these sensitive thick SOI structures containing sidewall doping and high-dose buried implants.

ACKNOWLEDGMENTS

We are grateful to Allan Pidduck of QinetiQ and Dieter Gräf of Wacker Siltronic for useful discussions.

REFERENCES

(1) Q.-Y. Tong and U. Gösele, *Semiconductor Wafer Bonding: Science and Technology*, Wiley Interscience, New York (1999).

(2) X. Cao, D. Nicholson, W.A. Nevin, and J. Knopke, in *Proceedings of the ECS Symposium on Crystalline Defects and Contamination: Their Impact and Control in Device Manufacturing (DECON 2001), Nuremberg, Germany, Sept., 2001.*

(3) W.A. Nevin, K. Somasundram, S. Blackstone, S. Magee, and A.T. Paxton, in *High Purity Silicon VI/2000*, C.L. Claeys, P. Rai-Choudhury, M. Watanabe, P. Stallhofer, and H.J. Dawson, Editors, PV 2000-17, p. 524, The Electrochemical Society Proceedings Series, Pennington, NJ (2000).

(4) H. Baumgart, T.J. Letavic, I. De Wolf, L. Tsou, H.E. Maes and R. Egloff, in *Semiconductor Wafer Bonding: Science, Technology and Applications III/1997*, U. Gösele, H. Baumgart, T. Abe, C. Hunt, and S. Iyer, Editors, PV 97-36, p. 440, The Electrochemical Society Proceedings Series, Pennington, NJ (1998).

(5) C.S. Cowen, D.R. Craven, C.A. Goodwin, C.-M. Hsieh, G.T. Jones, and T. Pandhumsoporn, *in Silicon-on-Insulator Technology and Devices VII/1996*, P.L.F. Hemment, S. Cristoloveanu, K. Izumi, T. Houston, and S. Wilson, Editors, PV 96-3, p. 364, The Electrochemical Society Proceedings Series, Pennington, NJ (1996).

(6) P. Papakonstantinou, K. Somasundram, X. Cao, and W.A. Nevin*, J. Electrochem. Soc.*, 148, G36 (2001).

(7) C. Gormley, K. Yallup, W.A. Nevin, J. Bhardwaj, H. Ashraf, P. Huggett, and S. Blackstone, in *Semiconductor Wafer Bonding: Science, Technology and Applications V/1999*, C.E. Hunt, H. Baumgart, T. Abe, and U. Gösele, Editors, PV 99-35, p. 350, The Electrochemical Society Proceedings Series, Pennington, NJ (2000).

SCHEME 1. Trench refill, annealing and slip inspection sequence.

sidewall TEOS liner deposition
↓
slip inspection
↓
1 h anneal at 1050ºC in nitrogen (liner densfication)
↓
slip inspection
↓
polysilicon refill
↓
planarisation of polysilicon
↓
slip inspection
↓
0.2 μm blanket TEOS deposition
↓
2 x 1 h anneals at 1050ºC in nitrogen (final densification)
↓
surface defect etch and slip inspection
↓
cross-sectional defect etch

TABLE I. Dependence of slip generation on arsenic buried implant dose and growth method of device material used for SOI fabrication, in 20 μm thick trenched and filled samples with a 0.6 μm thick TEOS oxide liner.

Oxygen concentration (atoms/cm^3)	Growth type	Implant dose (As ions/cm^2)	Degree of Slip (%)		
			Liner dep.	Liner dens.	Final dens.
7×10^{17}	CZ	0	0	0	0
7×10^{17}	CZ	3×10^{13}	0	0	0
7×10^{17}	CZ	5×10^{15}	0	0	0
$<10^{16}$	FZ	0	0	0	0
$<10^{16}$	FZ	3×10^{13}	0	0	0
$<10^{16}$	FZ	5×10^{15}	0	100	100

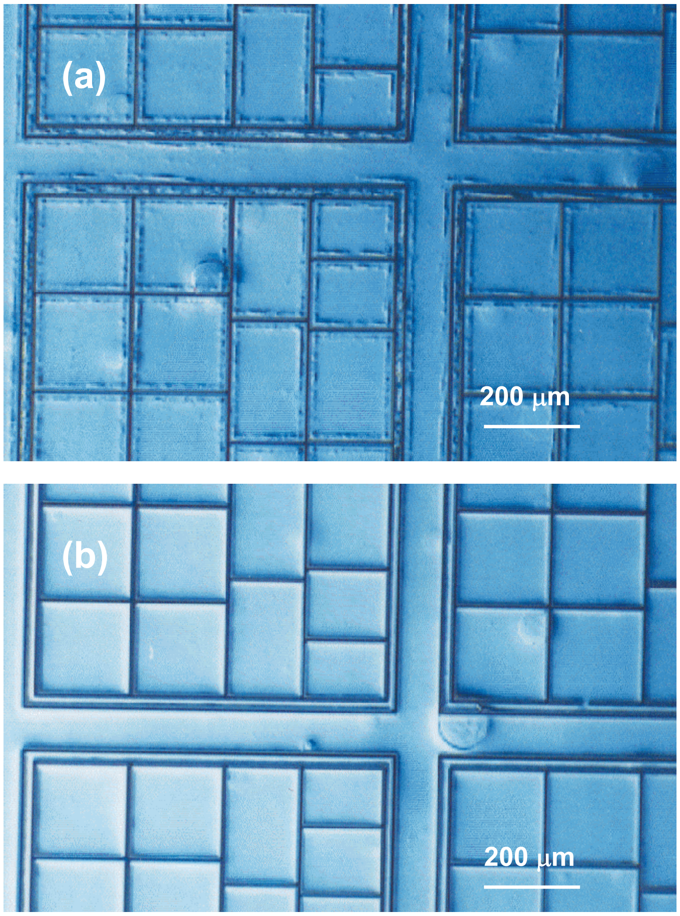

Fig. 1. Nomarski images of the Secco-etched surfaces of trenched SOI samples:
(a) with slip, and (b) without slip dislocations.

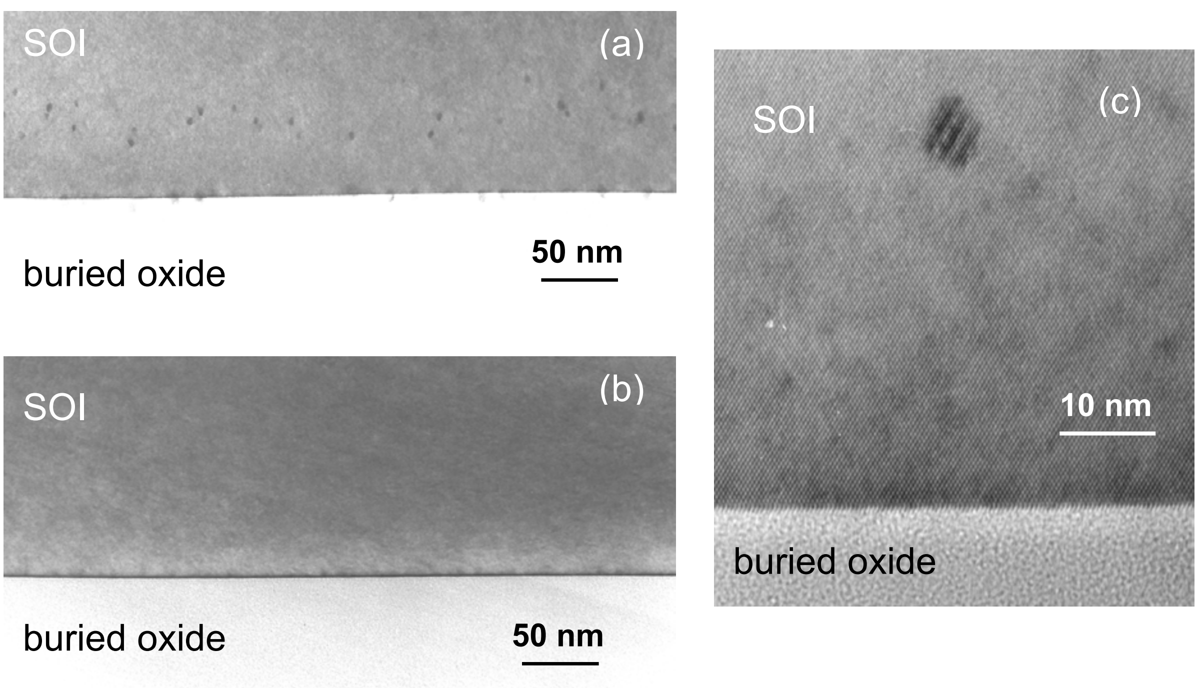

Figure 2. Cross-sectional TEM images of the interfaces of trenched SOI samples with (a) heavy-dose, and (b) light-dose arsenic implants. (c) shows a high resolution image of a crystalline precipitate.

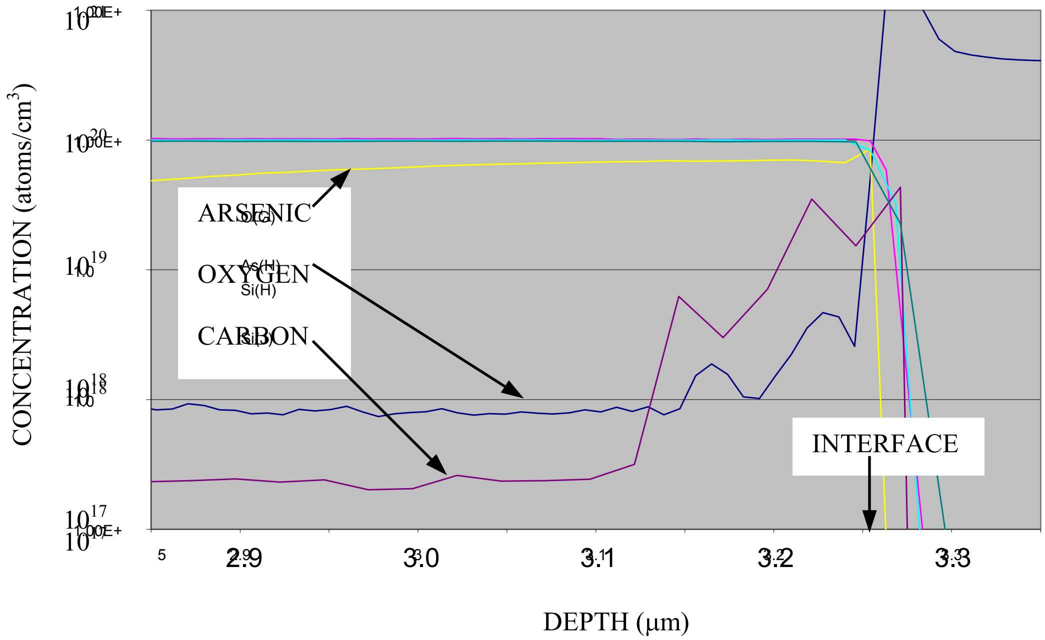

Figure 3. High-resolution SIMS profile through the SOI layer near the buried oxide interface of a sample with a heavy-dose arsenic implant.

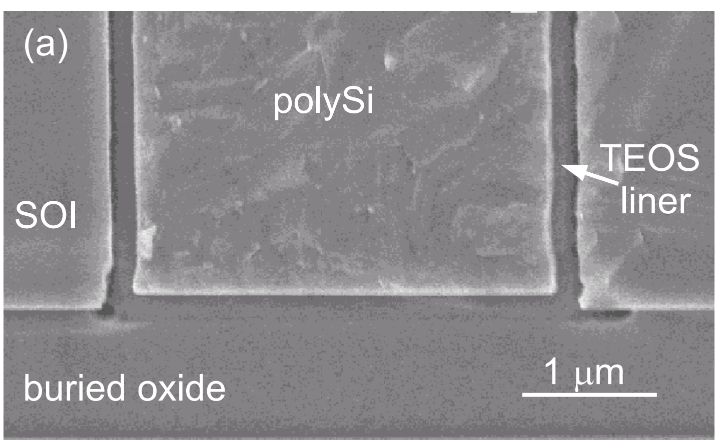

Fig. 4. SEM images of the trench bottom of trenched and filled SOI samples: (a) without and (b) with undercutting of silicon.

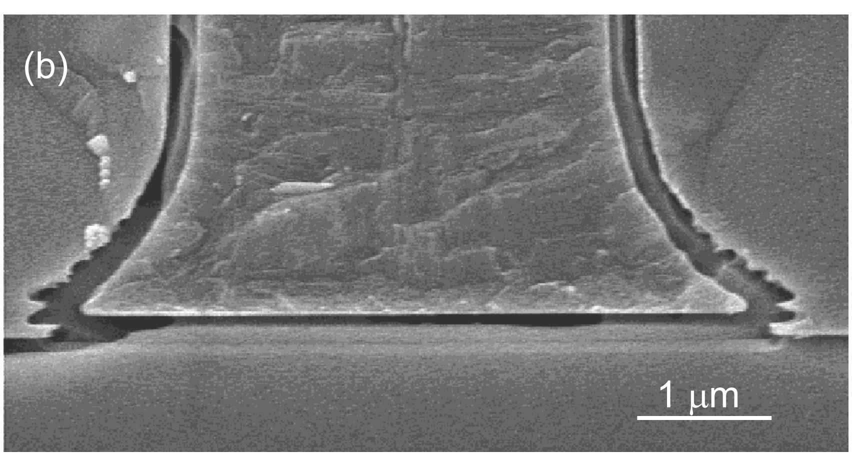

TABLE II. Dependence of slip generation on phosphorous sidewall doping level in trenched and filled SOI with a 0.8 μm thick oxide liner.

Dopant dose (P atoms/cm^2)	Degree of Slip (%) Liner dep.	Liner dens.	Final dens.
0	0	0	0
8×10^{14}	0	0	0
3×10^{15}	0	20	70
1×10^{16}	0	65	95

SOI = 20 μm, CZ

TABLE III. Dependence of slip generation on SOI thickness and TEOS oxide liner thickness in trenched and filled SOI samples.

SOI type	SOI material	SOI thickness (μm)	Liner thickness (μm)	Degree of Slip (%) Liner dep.	Liner dens.	Final dens.
A	CZ	20	0.9	0	0	2
A	CZ	30	0.9	0	0	5
A	CZ	50	0.9	0	0	35
A	CZ	20	0.7	0	0	0
A	FZ	20	0.7	0	0	0
A	FZ	20	0.9	0	0	0
A	CZ	20	1.2	0	1	5
A	FZ	20	1.2	0	2	5
B	CZ	35	0.25	0	0	0
B	CZ	35	0.30	0	3	5
B	CZ	35	0.35	0	33	60
C	CZ	35	0.55	0	0	0

SOI material = n-type (phos), (100) with sidewall doping;
Type A = unimplanted; Type B = 5×10^{15} ions/cm^2 As buried implant;
Type C = as B, but with pre-bond treated device wafer.